IEEE Access
Multidisciplinary | Rapid Review | Open Access Journal

Received September 12, 2018, accepted October 17, 2018, date of publication October 29, 2018,
date of current version December 7, 2018.

Digital Object Identifier 10.1109/ACCESS.2018.2878314

Multi-Objective Design Optimization of a Hexa-Rotor With Disturbance Rejection Capability Using an Evolutionary Algorithm

VICTOR MANUEL ARELLANO-QUINTANA[1], EDGAR ALFREDO PORTILLA-FLORES[2], AND EMMANUEL ALEJANDRO MERCHÁN-CRUZ[1]

[1]Instituto Politécnico Nacional-ESIME Azcapotzalco, Mexico 02250, Mexico
[2]Instituto Politécnico Nacional-CIDETEC- Grupo de Investigación e Innovación en Mecatrónica (GIIM), Mexico 07700, Mexico

Corresponding author: Victor Manuel Arellano-Quintana (e-mail: varellanoq1500@alumno.ipn.mx)

This work was supported in part by the Instituto Politécnico Nacional of México through the Secretaría de Investigación y Posgrado under Project SIP-20160672 and in part by COFAA. The work of V. M. Arellano-Quintana was supported by CONACYT.

ABSTRACT In this paper, a methodology to design a hexa-rotor with the capability to reject disturbances using tilted propellers is presented. The methodology proposes the use of a robustness index as a measurement of the capability to reject external disturbances. Moreover, an energy index is proposed as a measurement of the energy consumed by the hexa-rotor in hovering. It is shown that the robustness index is opposed to this energy index. Therefore, a multi-objective optimization problem is proposed in which the objective functions are the robustness index and the energy index. This problem is solved with the help of an evolutionary algorithm with a Pareto approach. Three solutions are selected from the Pareto front and tested with a proposed controller in order to show the feasibility of the methodology. Finally, the design that has a better tradeoff between the two objectives is simulated with Gaussian noise and with the maximum disturbance that is capable of rejecting.

INDEX TERMS Design optimization, evolutionary algorithms, aerial robotics, multi-objective optimization, robust design.

I. INTRODUCTION

In the recent years, the Unmanned Aerial Vehicles (UAV's) applications with multirotors have been widely increased for two main reasons, the easiness of construction and their relatively inexpensive components, [1]. In a standard multirotor all the rotors are oriented in the same direction, generating forces along the vertical axis, along with moments about roll, pitch and yaw axes. This configuration leads to an underactuated design, i.e. it has six degrees of freedom and four control inputs, independently of the number of the actuators. This configuration is well known because of its lack of robustness. However, this has not been a problem for people who work with them, control laws that deal with this underactuated nature have been developed and tested successfully in real-life applications, [2].

The standard configuration besides being simple it is also efficient in terms of energy since most of the time the multirotor is hovering, the propellers pointing vertically is an efficient configuration. Nevertheless, this advantage is bad for multirotor robustness since it is not possible to produced any force in the $x - y$ plane to mitigate forces. In order to reject such disturbances, attitude changes are needed, leading to losing the position and/or attitude and eventually becoming unstable.

Applications in which it is extremely important that the multirotor maintains its position precisely in a range of environmental conditions have grown in the last decades, such as, inspections, close-range spraying or aerial manipulation, [3]–[5]. However, perturbations due to turbulent wind or external forces/torques in physical interaction tasks, have to be compensated by the multirotor. Hence, in order to overcome these problems, some controllers have been developed [6]–[8], however, they are limited by the performance of the motors and their controllers; multirotor moment of inertia, and other factors.

Therefore in this paper, we proposed a methodology to design a hexa-rotor with disturbance rejection capability based on the principle of tilting rotors. Multirotors with tilted

rotors are capable of producing forces in the $x-y$ plane without needing a change in their attitude. This configuration has been studied in the last years, for instance, designs that are able to actively tilt their propellers [9], [10] and designs in which the propellers orientation is fixed, [11]–[13]. In the first case, the design leads to a waste of energy since it requires extra motors and extra mechanisms resulting in extra weight. In the fixed-tilted case, the design process has been relaxed since mathematical programming techniques have been used, i.e. parametrized the six propellers with only two angles instead of twelve, using one objective at the time, i.e. minimizing the control effort or maximizing the manipulability index. Hence, in this paper, we solve a multi-objective optimization problem with the help of evolutionary algorithms, parameterizing each propeller orientation with two angles and considering two objectives.

The main contributions of the paper are the following: a) We proposed a robustness index based on the radius of the maximum ball inside of the set of attainable forces and torques; b) We show that the robustness index proposed is opposed to the energy consumption in hovering; c) We propose a multi-objective problem to design a fully-actuated hexa-rotor having as design variables the twelve angles, two angles for each propeller; and d) We solve the problem with a Pareto approach and with the help of an evolutionary algorithm.

The paper is organized as follows, in Section II, some definitions are given that will help to understand better the robustness index proposed; in Section III the description of the n-motors multirotor is given; in Section IV, the robust index proposed is described together with the statement and solution of an optimization problem to maximize it; in Section V, the multi-objective problem is proposed and solved, and the description of the evolutionary algorithm used is given; in Section VI, simulations of three different designs are presented; in Section VII, the discussion of the results are presented giving some guidelines to rate the overall performance of the designs; finally the conclusions are given.

II. DEFINITIONS

Some definitions that will help to understand the proposed robustness index are given.

Definition 1: A half-space in $\mathbb{R}^n$ is a set of the form

$$\mathcal{H} = \{\mathbf{x} \in \mathbb{R}^n \mid \mathbf{a}^T\mathbf{x} \leq b\},$$

where $\mathbf{a} \in \mathbb{R}^n$, $b \in \mathbb{R}$, $||\mathbf{a}|| > 0$.

Definition 2: A convex set

$$\mathcal{P} = \{\mathbf{x} \in \mathbb{R}^n \mid \mathbf{P}\mathbf{x} \leq \mathbf{p}\},$$

with $\mathbf{P} \in \mathbb{R}^{n_p \times n}$, $\mathbf{p} \in \mathbb{R}^{n_p}$, $n_p < \infty$, is called polyhedron. A bounded polyhedron is called polytope. A polytope is the bounded intersection of n-closed half-spaces. Every projection of $\mathcal{P}$ is a polytope.

Definition 3: A polytope $\mathcal{P} = \{\mathbf{x} \in \mathbb{R}^n \mid \mathbf{P}\mathbf{x} \leq \mathbf{p}\}$ is full dimensional if it is possible to fit a non-empty n-dimensional ball of radius r and centered in $\mathbf{x}_c$ in $\mathcal{P}$, i.e.,

$$\exists\, \mathbf{x}_c \in \mathbb{R}^n, r > 0 \;:\; \mathcal{B}(\mathbf{x}_c, r) \subset \mathcal{P},$$

where

$$\mathcal{B}(x_c, r) := \{\mathbf{x} \in \mathbb{R}^n \mid ||\mathbf{x} - \mathbf{x}_c|| \leq r\}.$$

Definition 4: A Chebyshev ball of a polytope $\mathcal{P} = \{\mathbf{x} \in \mathbb{R}^n \mid \mathbf{P}\mathbf{x} \leq \mathbf{p}\}$ with $\mathbf{P} \in \mathbb{R}^{n_p \times n}$, $\mathbf{p} \in \mathbb{R}^{n_p}$, corresponds to the largest radius ball in $\mathbb{R}^n$ such that $\mathcal{B}(\mathbf{x}_c, r) \subset \mathcal{P}$.

III. DESCRIPTION OF THE SYSTEM

The dynamics of an n-rotor can be described by the following matrix equation,

$$\underbrace{\begin{bmatrix} m\mathbf{I}_3 & \mathbf{0}_3 \\ \mathbf{0}_3 & \mathbf{J} \end{bmatrix}}_{\mathbf{M}} \underbrace{\begin{bmatrix} \ddot{\mathbf{p}} \\ \dot{\boldsymbol{\omega}} \end{bmatrix}}_{\mathbf{a}} = \underbrace{\begin{bmatrix} -mg\hat{\mathbf{z}} \\ -\boldsymbol{\omega} \times \mathbf{J}\boldsymbol{\omega} \end{bmatrix}}_{\mathbf{f}} + \underbrace{\begin{bmatrix} \mathbf{R}_r & \mathbf{0}_3 \\ \mathbf{0}_3 & \mathbf{I}_3 \end{bmatrix}}_{\mathbf{B}} \underbrace{\begin{bmatrix} \mathbf{F}_1 \\ \mathbf{F}_2 \end{bmatrix}}_{\mathbf{F}} \mathbf{u} \tag{1}$$

where n is the number of rotors; m is the multirotor mass; $\mathbf{J}$ is the multirotor moment of inertia; $\mathbf{p}$ is the multirotor position w.r.t. inertial frame; ω is the velocity about roll, pitch and yaw w.r.t. the body frame; g is the gravity acceleration; $\mathbf{R}_r$ is the rotation matrix that maps from the body frame to the inertial frame; $\hat{\mathbf{z}}$ is defined as $\hat{\mathbf{z}} = [0, 0, 1]^T$; and $\mathbf{u}$ is the control input vector. In this work we are interested in designing a hexa-rotor i.e. $n = 6$. In Figure 1, the hexa-rotor with tilted propellers is shown.

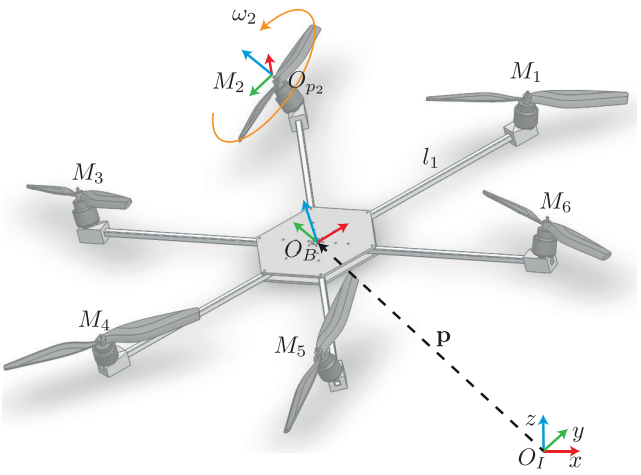

FIGURE 1. Hexa-rotor description. O_I is the inertial frame; O_B is the frame attached to the body and coincides with the center of mass (CoM); O_{p_i} is the frame attached to a propeller i; M_i is the motor number i; $\mathbf{p}$ is the position vector, and l_1 is the length of the arm i, all the arms have the same length.

ALLOCATION MATRIX F

Matrix $\mathbf{F}$ is the allocation matrix of the total wrench applied to the multirotor; matrices $\mathbf{F}_1$ and $\mathbf{F}_2$ are the force and moment matrices, respectively. Matrix $\mathbf{F}_1 \in \mathbb{R}^{3\times n}$ is conformed of unit vectors $\mathbf{v}_i \in \mathbb{R}^{3\times 1}$ that define the orientation of the propeller i, $||\mathbf{v}_i|| = k_f$, where k_f is the coefficient that relates

the spinning velocity with the thrust. Matrix $\mathbf{F}_2 \in \mathbb{R}^{3\times n}$ is conformed of vectors $\mathbf{w}_i \in \mathbb{R}^{3\times 1}$ that define the sum of the torque due to thrust and the torque due to drag moment, i.e. $\mathbf{w}_i = k_m\sigma_i\mathbf{v}_i + \mathbf{r}_i \times \mathbf{v}_i$, where $\mathbf{r}_i$ is the position vector of propeller i to the center of gravity of the vehicle; k_m is a coefficient that relates the spinning velocity with the torque produced around the rotation axis, and σ_i is the direction of rotation $\sigma_i \in \{-1, 1\}$. To compensate the torque (drag moment) of each propeller the value of σ_i is defined as $\sigma_i = -1^i$.

On the other hand, matrix $\mathbf{F}_1$ conformed of vectors $\mathbf{v}_i$ can be parametrized by using two angles that will describe the propeller orientation. These two angles α_i and β_i are shown in Figure 2. This last will reduce the number of variables to be found by the optimization algorithm. Furthermore, in this work, we consider a couple of angles for each propeller of the hexa-rotor. A more detailed description of these angles can be found in [12] and [14].

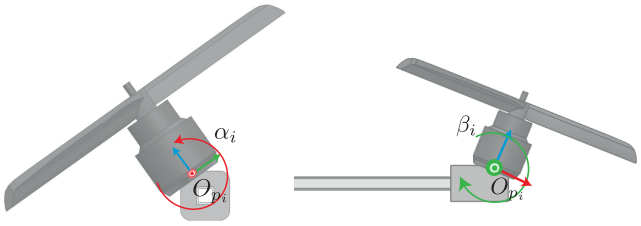

FIGURE 2. Propellers frame parametrization with α_i and β_i angles.

IV. ROBUSTNESS INDEX

In order to design a hexa-rotor with the capability of disturbance rejection, we translate the robustness as the ball of radius r inside of the set of admissible forces and torques due to the saturation of the actuators centered in hovering. This ball represents the control authority over the hexa-rotor, and hence the capability to reject disturbances, the bigger the ball, the higher the robustness.

The set of admissible forces and torques can be represented in terms of the saturated inputs $u_{i,lb} \leq u_i \leq u_{i,ub}$. The control input $\mathbf{u}$ defined in Section III is a polytope, Definition 2, and its H-representation is the following,

$$\mathcal{U} = \{\mathbf{x} \in \mathbb{R}^n \mid \mathbf{C}_U\mathbf{x} \leq \mathbf{b}_u\} \tag{2}$$

where $\mathbf{C}_U \in \mathbb{R}^{m\times n}$, $m = 2n$ since all the actuators are saturated, and $\mathbf{C}_U = \begin{bmatrix}\mathbf{I}_{n\times n} & -\mathbf{I}_{n\times n}\end{bmatrix}^T$.

Since the total wrench $\mathbf{W} = \mathbf{F}\mathbf{u}$ is the image of $\mathcal{U}$ trough the linear transformation $\mathbf{F}$, it turns out that $\mathbf{W}$ is also a polytope [15], and its H-representation is the following,

$$\mathcal{W} = \{\mathbf{x} \in \mathbb{R}^n \mid \mathbf{C}_W\mathbf{x} \leq \mathbf{b}_w\} \tag{3}$$

where $\mathbf{C}_W \in \mathbb{R}^{m\times n}$, $m = 2n$.

Thus for finding the maximum ball inscribed into $\mathcal{W}$ we refer to the Chebyshev ball, Definition 4. If $\mathbf{F}$ is no singular then $\mathbf{C}_W = \mathbf{C}_U\mathbf{F}^{-1}$ and $\mathbf{b}_w = \mathbf{b}_u$, otherwise $\mathcal{W}$ is empty.

The Chebyshev ball will be centered in $\mathbf{w}^*$ that corresponds to the virtual inputs (desired forces and torques), i.e. $\mathbf{u} = \mathbf{F}^{-1}\mathbf{w}^* = \mathbf{F}^{-1}\begin{bmatrix}0, 0, mg, 0, 0, 0\end{bmatrix}^T$ in case of hovering.

The maximum ball of radius r can be found by solving the following LP problem, [16],

$$\begin{aligned} &\max_{\mathbf{x}_c, r} \ r \\ &\text{s.t. } \mathcal{B}(\mathbf{x}_c, r) \subset \mathcal{W} \\ &\qquad r > 0 \end{aligned} \tag{4}$$

However, this LP problem considers that the polytope $\mathcal{W}$ is already defined. Therefore, the values of this polytope have to be found by the algorithm in order to find the maximum ball of radius r inscribed in the polytope. Problem (4) can be rewritten considering the propellers angles α_i and β_i, as follows:

$$\begin{aligned} &\max_{\alpha_i, \beta_i, r} \ r \\ &\text{s.t. } \mathbf{C}_{W_i}\mathbf{w}^* + r||\mathbf{C}_{W_i}|| \leq \mathbf{b}_{u_i}, \ i = 1, \ldots, m \\ &\qquad -\frac{\pi}{2} < \alpha_i < \frac{\pi}{2}, \qquad i = 1, \ldots, n \\ &\qquad -\frac{\pi}{2} < \beta_i < \frac{\pi}{2}, \qquad i = 1, \ldots, n \\ &\qquad r > 0 \end{aligned} \tag{5}$$

One way to solve problem (5) could be by solving many LP problems (4) with different combinations of angles α_i and β_i, and finding which combination gives the maximum value of r. This method will lead to calculate at least 4.7383×10^{30} possible combinations with 0.5 deg of accuracy in the interval $(-\pi/2, \pi/2)$, if the six propellers are parametrized with only two angles instead of twelve, the number of combinations will be reduced to 1.2960×10^5 possible combinations, with the same accuracy.

Therefore, to solve problem (5), we resort to optimal stochastic algorithms, such as evolutionary algorithms. These algorithms characterize because they do not need any gradient or Hessian information. One of the most famous EA is the Genetic Algorithm (GA). However, GA might present local minima problem [17], [18], so, further studies using a different approach have been developed, such as Differential Evolution (DE) algorithm proposed in [19] as a continuous unconstrained single-objective optimization algorithm. A substantial number of papers have been produced since, showing its good performance as well as the number of objective function evaluations, [20], [21].

A. SINGLE-OBJECTIVE DIFFERENTIAL EVOLUTION ALGORITHM

The basic principle of DE algorithm relies on the design of a simple mutation operator based on the linear combination of three different individuals and on a crossover step that mixes the initial and the mutated solutions. The algorithm was designed for unconstrained problems, however, a constraint manager can be used, for instance, Deb rules [22] or stochastic ranking [23]. In Algorithm 1 the single-objective DE

Algorithm 1 Single-Objective Differential Evolution

$G = 0$;
Create a random initial population $\overrightarrow{x}_i^G, \forall i = 1, \ldots, NP$;
Evaluate each $\overrightarrow{x}_i^G$ in the objective function $f(\overrightarrow{x}_i^G)$ and in each constraint, $\forall k = 1, \ldots, NP.$;
for $G = 1$ *to* G_{Max} **do**
  for $i = 1$ *to* NP **do**
    Select randomly $r_1 \neq r_2 \neq r_3$ from the current population;
    $j_{rand} = randint(1, X)$;
    for $j = 1$ *to* X **do**
      if $rand_j(0, 1) < CR \,||\, j = j_{rand}$ **then**
        $u_{i,j}^{G+1} = x_{r3,j}^G + F(x_{r1,j}^G - x_{r2,j}^G)$;
      else
        $u_{i,j}^{G+1} = x_{i,j}^G$
      end
    end
    Evaluate $\overrightarrow{u}_i^{G+1}$ in the objective function $f(\overrightarrow{u}_i^G)$ and in each constraint.;
    Evaluate Deb rules.
  end
  $G = G + 1$
end

algorithm using Deb rules as constraints manager is shown. The nomenclature is the following: NP is the number of individuals in the population; X is the number of design variables; CR is the crossover probability; F is the mutation factor; G_{Max} is the maximum number of generations.

B. RESULTS MAXIMUM ROBUSTNESS INDEX

Problem (5) was solved using DE algorithm and Deb rules as constraint manager. The algorithm parameters used are shown in Table 1 together with the physical properties of the platform obtained from a CAD model. The problem was solved in hovering, and vector of the desired forces/torques was the following $\mathbf{w}^* = \left[0, 0, mg, 0, 0, 0\right]^T$. After solving problem (5), the maximum robustness index found by the algorithm was $r^* = 4.4981$, and the α_i and β_i of each propeller found by the algorithm are gathered in Table 2. The hexa-rotor configuration is shown in Figure 4.

TABLE 1. Algorithm parameters and platform properties.

Parameter	Value	Parameter	Value
NP	150	CR	0.5
F	0.2	G_{Max}	5000
C_e	0.5	m	1.3 kg
u_{lb}	256 Hz^2	u_{ub}	16 900 Hz^2

Despite the ball of attainable forces and torques belongs to a six-dimensional space, we can find the maximum ball of attainable forces in a three-dimensional space, this maximum

TABLE 2. Angles found by solving problem (5).

Angle	Value [deg]	Angle	Value [deg]
α_1	68.60	β_1	34.89
α_2	−76.02	β_2	−33.38
α_3	64.81	β_3	32.78
α_4	−68.88	β_4	−47.20
α_5	68.01	β_5	42.34
α_6	−73.42	β_6	−41.17

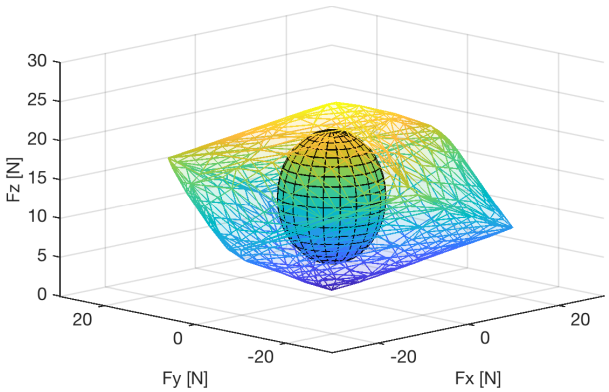

FIGURE 3. Ball of attainable force enclosed by the polytope of the saturated inputs.

ball can be found by solving an LP problem similar to (4) but in a three-dimensional space. The last is possible since matrix $\mathbf{F}$ is non-singular, therefore, forces and torques are independent. The maximum ball of the attainable forces centered in hovering is shown in Figure 3, the ball is inside of the polytope generated by the actuators.

C. ENERGY EFFICIENCY

However, the propellers configuration in Table 2 is not energy efficient. From aerodynamics, it is known that the required power to drive the propeller is proportional to the cube of its spinning speed, i.e. $P \approx \omega^3$, [24]. Hence, it can be said that if the propeller velocity is minimized, the power required by the propeller will also be minimized; this can be seen also from the drag, that it is the motor load and constitutes a power dissipation element. The drag is proportional to the square of the velocity $Q \approx \omega^2$, therefore, if the velocity is minimized, the drag will be minimized.

In order to show the energy consumption of the hexa-rotor in hover mode we propose the following energy index,

$$J_e = ||\mathbf{F}^{-1}\mathbf{w}^*||_2 = ||\mathbf{u}||_2. \tag{6}$$

A comparison of the energy index can be made to show the energy efficiency between the tilted hexa-rotor found by the algorithm and a standard hexa-rotor. The propellers of a standard hexa-rotor are coplanar and collinear, this is the most efficient configuration in terms of energy for hovering. However, such configuration is not capable of producing thrust in $x - y$ plane, in other words, the ball radius of attainable forces/torques and therefore, the robustness index

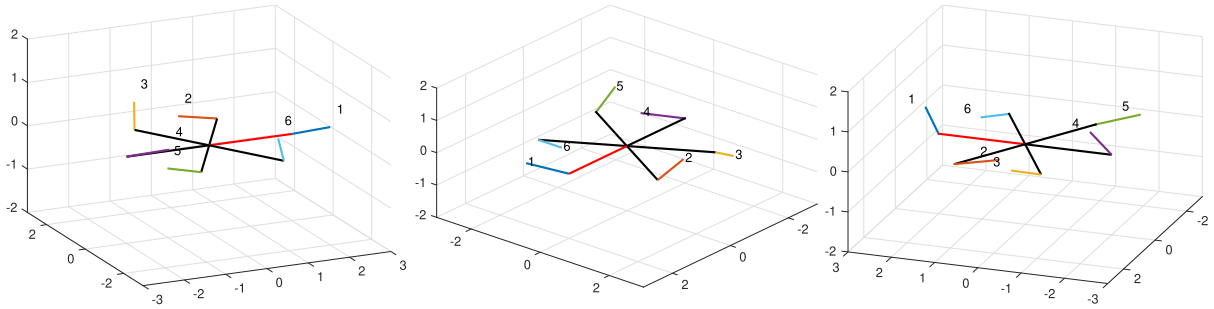

FIGURE 4. Hexa-rotor configuration found for maximum robustness index, different perspectives. The red arm indicates the x axis.

TABLE 3. Angles found by the three solutions along the Pareto front.

Solution	α_1	α_2	α_3	α_4	α_5	α_6	β_1	β_2	β_3	β_4	β_5	β_6
i	−62.54	62.98	−63.23	63.65	−63.06	63.60	1.12	3.33	−0.17	1.70	1.74	0.16
ii	−39.31	35.40	−39.94	39.88	−34.05	38.98	0.34	−1.86	−5.37	−1.01	−4.64	0.04
iii	−13.39	16.40	−15.10	12.89	−16.23	1.81	0.96	−0.16	5.19	−1.06	1.44	0.00

is theoretically zero (it can be different from zero due to imperfections in the propellers attachments). On the other hand, the configuration found by the algorithm wastes $\approx 26\,\%$ more energy to hover. It is clear that the two aspects, i.e. the robust index and the energy index proposed are opposed. Hence, a multi-objective problem arises, in which the energy index J_e can be considered as the second objective.

V. MULTI-OBJECTIVE OPTIMAL PROBLEM

To solve a multi-objective problem, there are some approaches to find the better trade-off between two or more objectives. For instance, by using a weighted cost function, i.e. $F = \alpha_1 f_1 + \alpha_2 f_2$ where $\alpha_1, \alpha_2 > 0$. However, this approach transforms the multi-objective problem into a single-objective problem which is not desirable because the solution will depend on the weight values, this means that each combination of weights will lead to one optimal solution instead of a set of optimal solutions. Therefore, a different approach will be used in this work, based on non-dominated solutions along the Pareto front. This approach allows to find as many solutions as the algorithm is capable of finding, and from which the design engineer can choose from according to the application requirements.

A. OPTIMIZATION PROBLEM

The problem of finding the maximum ball radius and the minimum energy index can be considered as a multi-objective problem because both objectives are opposed as it was shown in the previous section, i.e. if the robustness index r increases, the energy index J_e increases and vice-versa. Therefore, the multi-objective problem that considers both objectives can be stated as,

$$\begin{aligned} &\underset{\alpha_i,\beta_i,r}{\text{optimize}} \ \boldsymbol{\Phi} \\ &\text{s.t. } \mathbf{C}_{W_i}\mathbf{w}^* + r||\mathbf{C}_{W_i}|| \leq \mathbf{b}_{u_i}, \ i = 1,\ldots,m \\ &-\frac{\pi}{2} < \alpha_i < \frac{\pi}{2}, \quad i = 1,\ldots,n \\ &-\frac{\pi}{2} < \beta_i < \frac{\pi}{2}, \quad i = 1,\ldots,n \\ &r > 0 \end{aligned} \tag{7}$$

where $\boldsymbol{\Phi}$ is a vector that contains the objective functions, i.e. $\boldsymbol{\Phi} = \left[r, J_e\right]^T$. Notice that the first objective r is to be maximized and the second objective J_e is to be minimized.

This optimization problem can be solved with a multi-objective version of the DE algorithm presented in Algorithm 1, the aim is to find a set of optimal solutions that hold the Pareto optimality leading to a Pareto front in which a solution that fits better with the requirements can be selected and analyzed. These requirements are the robustness index and the energy index. Hence, to solve problem (7), we resort to the multi-objective algorithm based on DE.

B. MULTI-OBJECTIVE EVOLUTIONARY ALGORITHM

Problem (7) can be solved with a multi-objective algorithm based on DE algorithm presented in Section IV-A. However, some changes have to be done in order to handle both objectives with their constraints. Unlike using the criteria to select the fittest solution between parent and offspring in traditional DE; in multi-objective optimization, the algorithm is looking for non-dominated solutions. However, since the problem (7) has constraints, the following non-dominated rules are used to find solutions along the Pareto front,

- Between two feasible solutions, the one that dominates the other wins.
- If one solution is feasible and the other one is infeasible, the feasible individual wins.
- If both solutions are infeasible, the one with the lower sum of constraint violation wins.
- If the two solutions are feasible and non-dominated, the first wins if $rand(0, 1) > C_e$, otherwise, the second wins.

TABLE 4. Parameters used with the multi-objective DE algorithm.

Parameter	Value	Parameter	Value
NP	100	CR	0.75
F	0.5	G_{Max}	10 000
C_e	0.5	Mass	1.3 kg
u_{lb}	256 Hz^2	u_{lb}	16 900 Hz^2

Algorithm 2 Multi-Objective Differential Evolution

$G = 0$;
Initialize the external memory $EM_0 = \emptyset$;
Create a random initial population $\overrightarrow{x}_i^G, \forall i = 1, \ldots, NP$;
Evaluate each $\overrightarrow{x}_i^G$ in each objective function $f_k(\overrightarrow{x}_i^G)$ and in each constraint, $\forall k = 1, \ldots, NP$. ;
Evaluate the non-dominated rules in search of feasible-non-dominated solutions to add to the EM.;
for $G = 1$ *to* G_{Max} **do**
  for $i = 1$ *to* NP **do**
    if $C_{cr}G_{Max} \geq G$ && $EM_G \geq 3$ **then**
      Select randomly $r_1 \neq r_2 \neq r_3$ from the EM;
    else
      Select randomly $r_1 \neq r_2 \neq r_3$ from the current population;
    end
    $j_{rand} = randint(1, X)$;
    for $j = 1$ *to* X **do**
      if $rand_j(0, 1) < CR \,||\, j = j_{rand}$ **then**
        $u_{i,j}^{G+1} = x_{r_3,j}^G + F(x_{r_1,j}^G - x_{r_2,j}^G)$;
      else
        $u_{i,j}^{G+1} = x_{i,j}^G$
      end
    end
    Evaluate $\overrightarrow{u}_i^{G+1}$ in each objective function $f_k(\overrightarrow{u}_i^G)$ and in each constraint.;
    Evaluate the non-dominated rules in search of feasible-non-dominated solutions to add to the EM.;
  end
  $G = G + 1$ Find the non-dominated solutions ND_G from the current population: $\overrightarrow{x}_i^G, \forall i, i = 1, \ldots, NP$;
  Update EM_G with ND_G and verify non-dominance. ;
end

We took the DE algorithm presented in [19] using the non-dominated rules and the crowding operator from [25], also we promote elitism by implementing the External Memory (EM) proposed in [26]. This EM promotes elitism if a certain number of generations is reached, determined by the crowding factor C_{cr}. If the number of generations is reached, the algorithm will choose only those individuals that belong to this population (that actually is the Pareto front, since all the individuals are non-dominated) sorted by their crowding distance, by doing this, elitism allows finding solutions to fill the empty spaces along the Pareto front, the EM has to have at least three individuals to promote elitism. The algorithm used for solving the multi-objective problem is shown in Algorithm 2.

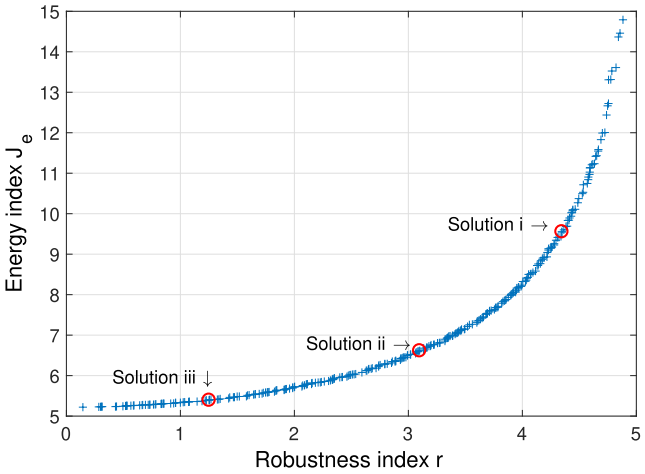

FIGURE 5. Pareto Front. Solutions i, ii and iii are encircled.

TABLE 5. Pareto front in descending order with respect to second objective J_e. Solution i, ii, iii are highlighted in red, green and blue, respectively.

Individual	First objective r	Second objective J_e
⋮	⋮	⋮
41	4.3990	9.8324
42	4.3931	9.6917
45	4.3471	9.5539
46	4.3464	9.5482
47	4.3389	9.4376
⋮	⋮	⋮
147	3.1650	6.6956
148	3.1594	6.6926
151	3.0991	6.6142
152	3.0860	6.6024
153	3.0836	6.5908
⋮	⋮	⋮
255	1.2551	5.4044
256	1.2541	5.3941
257	1.2519	5.3927
258	1.2278	5.3918
259	1.2177	5.3815
⋮	⋮	⋮

C. DESIGN RESULTS

Problem (7) was solved using multi-objective DE algorithm and non-dominated rules to handle the constraints. The algorithm parameters used are shown in Table 4 together with the physical properties of the platform. The problem was solved in hovering, and the vector of the desired forces/torques was the following $\mathbf{w}^* = \left[0, 0, mg, 0, 0, 0\right]^T$.

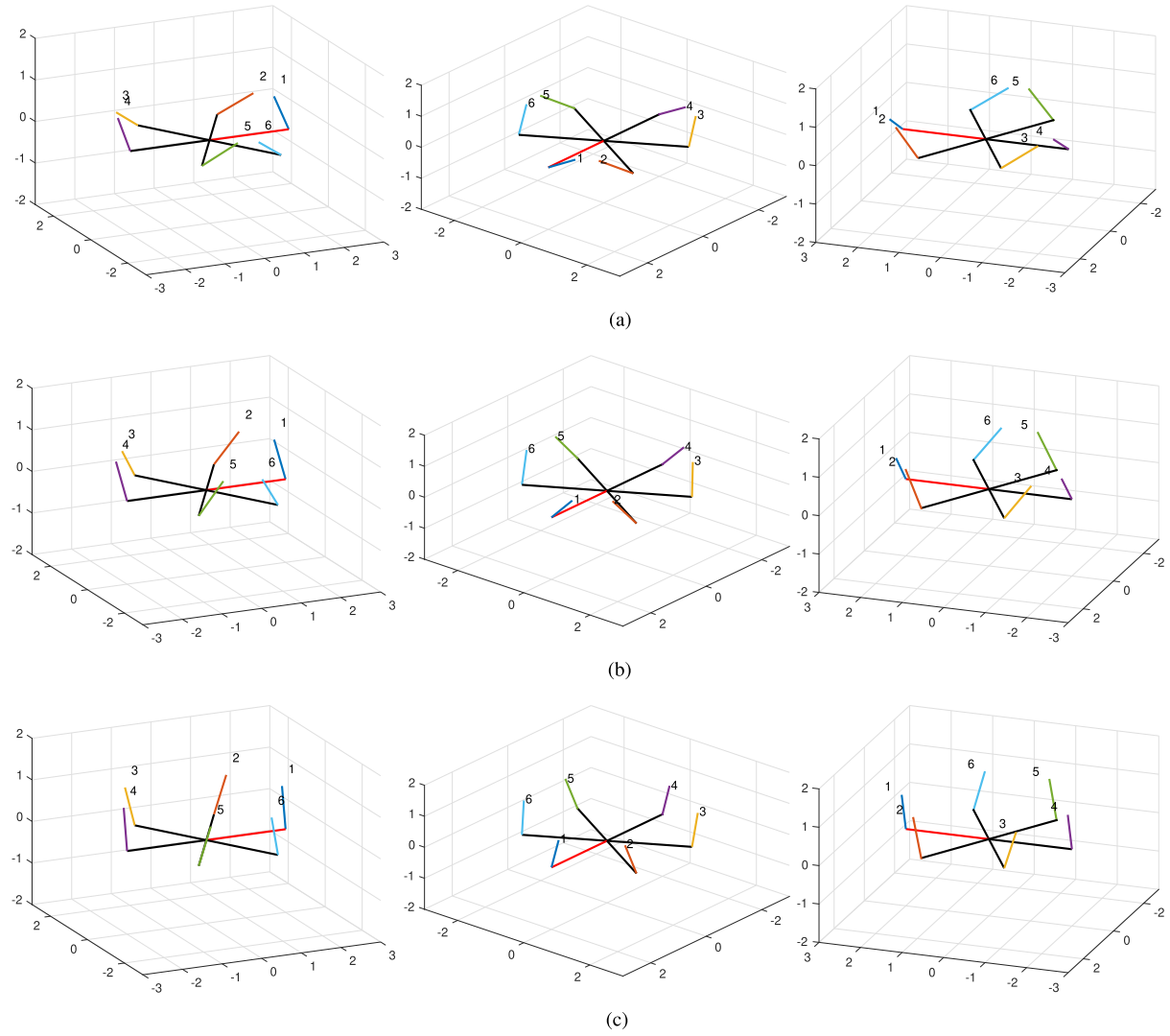

FIGURE 6. Hexa-rotor configurations of solutions i, ii and iii. The red arm indicates de x axis. (a) Different perspectives of solution i; Robustness index $r = 4.3471$, and Energy index $J_e = 9.5539$. (b) Different perspectives of solution ii; Robustness index $r = 3.0991$, and Energy index $J_e = 6.6142$. (c) Different perspectives of solution iii; Robustness index $r = 1.2519$, and Energy index $J_e = 5.3927$.

Pareto front of the solutions found by the algorithm is shown in Figure 5. The design engineer can select from this front the solution that better fits with the design goal. To analyze the front we can arrange the solutions in ascending/descending regardless of whether we choose the first or second objective. This arrangement is shown in a simplified manner in Table 5.

Table 5 can be divided into three regions from which three solutions can be taken equidistantly in order to analyze the designs, this method will allow choosing solutions that satisfy the following: the first one satisfies better the first objective but not the second; the second one is in the middle of the front (better trade-off), and the last one satisfies better the second objective but not the first.

The solutions selected from the Pareto front will be tested in order to verify the disturbance rejection capability and the energy consumption as well. Notice that the tilted propellers allow decoupling the translational and the rotational dynamics, as it is shown in [10] and [12]. Therefore, the solutions are capable of tracking a desired trajectory both in position and attitude independently. The propeller configuration of the three solutions are shown in Figure 6. In Table 3, the propeller configurations for each solution are gathered. Noticed, that β_i angles are close to zero values in contrast with the β_i values found by solving problem (5), this is mainly due to the second objective in which the energy index minimization is considered to find the optimal designs.

VI. SIMULATIONS RESULTS

The three selected solutions will be tested in simulations to examine the response against disturbances and to compute the energy index over time. The hexa-rotor is driven to a desired position (x_r, y_r, z_r) in horizontal position $(\phi_r = 0, \theta_r = 0, \psi_r = 0)$ and then while hovering an external force

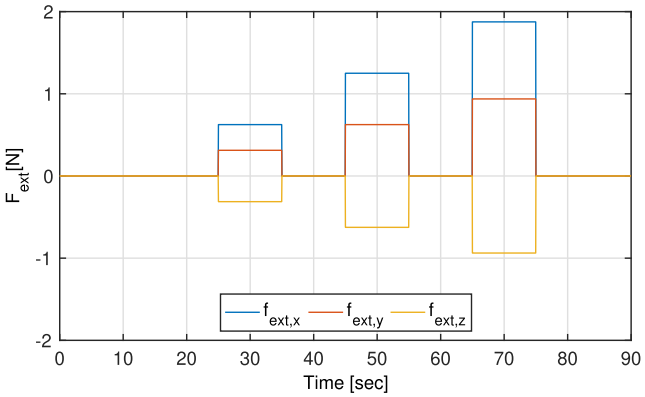

FIGURE 7. Disturbances applied to the hexa-rotor CoM at equidistant instants of time.

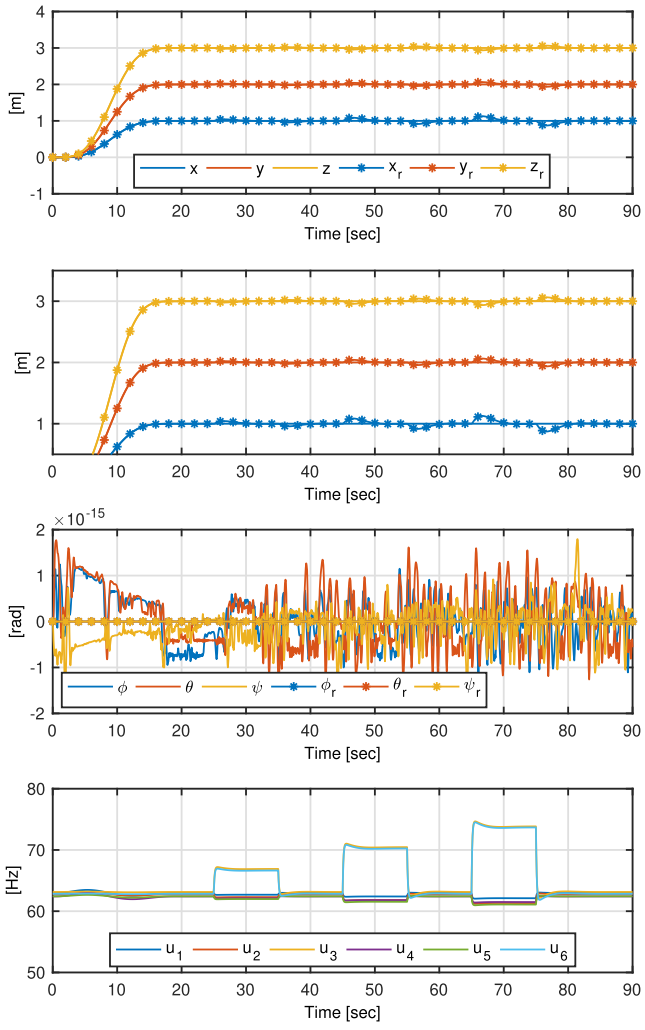

FIGURE 8. Simulations results with solution i. The dynamic energy index was equal to 8.9060×10^5.

with components in $x-y-z$ in inertial coordinates is exerted in the center of mass (CoM) of the hexa-rotor.

In theory, the controller is capable of compensating almost any disturbance as long as the control input is unbounded.

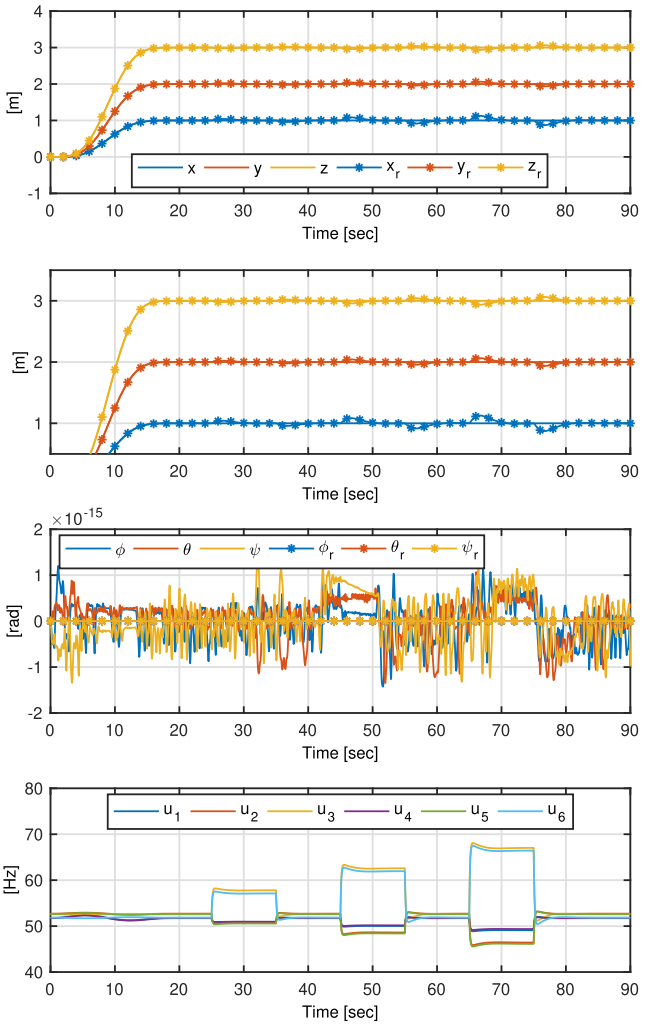

FIGURE 9. Simulations results with solution ii. The dynamic energy index was equal to 6.2161×10^5.

However, this is not the case, the control inputs are saturated, hence, the capability of disturbance rejection is highly dependent on the propellers configuration as it will be shown in the following.

The controller used in this simulations is a Feedback Linearization with a PID controller. The PID controller is defined as follows,

$$\mathbf{w}_d = -\mathbf{f} - \mathbf{K}_p\mathbf{e}_p - \mathbf{K}_d\dot{\mathbf{e}}_p - \mathbf{K}_i\int_{t_0}^{tf}\mathbf{e}_p dt + \mathbf{a}_d \tag{8}$$

where matrices $\mathbf{K}_p, \mathbf{K}_d, \mathbf{K}_i \in \mathbb{R}^{6\times 6}$ are diagonal matrices with proper proportional, derivative and integral gains, respectively; the errors in translation and orientation are defined as follows, [27],

$$\mathbf{e}_p = \begin{bmatrix}\mathbf{e}_{pos}\\ \mathbf{e}_{att}\end{bmatrix} = \begin{bmatrix}\mathbf{p}-\mathbf{p}_r\\ \frac{1}{2}(\mathbf{R}_d^T\mathbf{R}_r - \mathbf{R}_r^T\mathbf{R}_d)\end{bmatrix} \tag{9}$$

$$\dot{\mathbf{e}}_p = \begin{bmatrix}\dot{\mathbf{e}}_{pos}\\ \mathbf{e}_{\omega}\end{bmatrix} = \begin{bmatrix}\dot{\mathbf{p}}-\dot{\mathbf{p}}_r\\ \boldsymbol{\omega} - \mathbf{R}_r^T\mathbf{R}_d\hat{\boldsymbol{\omega}}_r\end{bmatrix} \tag{10}$$

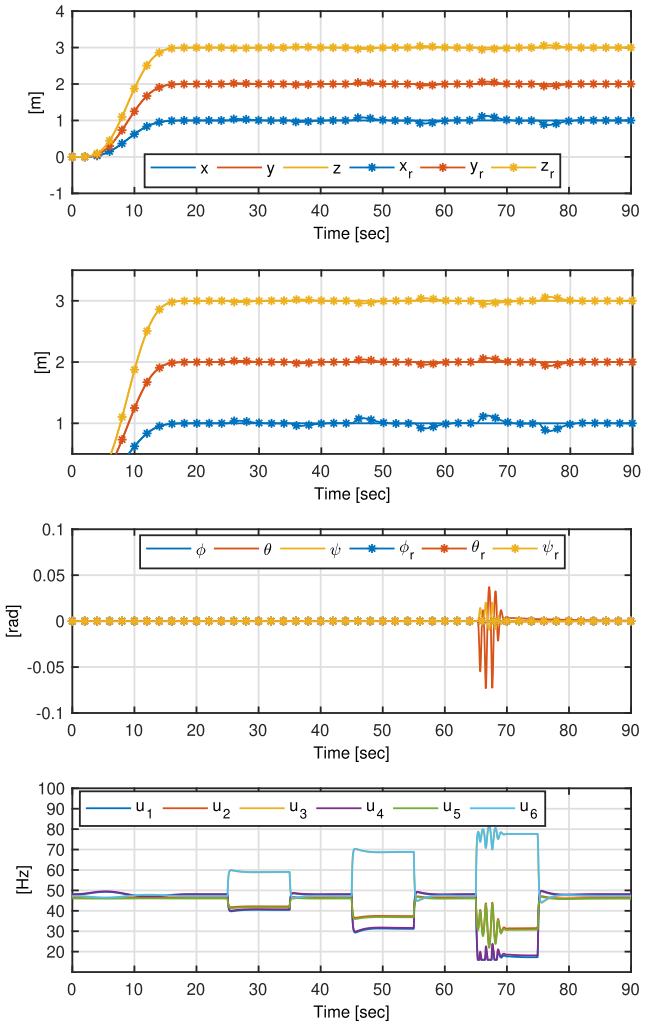

FIGURE 10. Simulations results with solution iii. The dynamic energy index was equal to 5.4396×10^5.

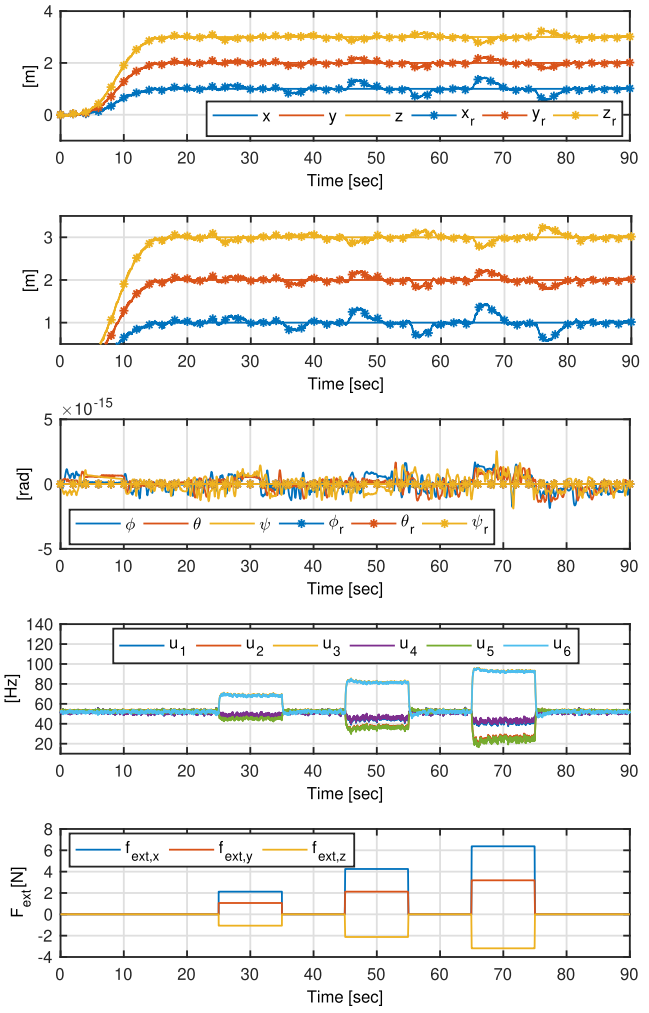

FIGURE 11. Simulations results of solution ii with Gaussian noise and maximum disturbance before becoming unstable. The dynamic energy index was equal to 7.0649×10^5.

where $\mathbf{p}_r$ is the desired position; $\mathbf{R}_d$ is the desired rotation matrix; $\hat{(.)}$ is the hat operator; $\boldsymbol{\omega}_r = \mathbf{R}_d^T \dot{\mathbf{R}}_d$.

The control allocation strategy is simple since the matrix $\mathbf{F}$ is full rank, the control allocation is made by just inverting it as follows,

$$\mathbf{u} = (\mathbf{M}^{-1}\mathbf{B}\mathbf{F})^{-1}\mathbf{w}_d. \tag{11}$$

The external disturbances are applied to the CoM with components in the three axes $F_{x_{ext}}, F_{y_{ext}}, F_{z_{ext}}$, as it is shown in Figure 7.

On the other hand, since we are interested in the energy consumption we defined the dynamic energy index as follows,

$$H = \int_{t_0}^{t_f} ||\mathbf{u}||_2 dt. \tag{12}$$

After carrying out the simulations with the three solutions selected from the Pareto front, the results are shown in Figures 8, 9 and 10.

VII. DISCUSSION

The three solutions chosen from the Pareto front are optimal in the Pareto sense, and the three are capable of rejecting the disturbances, as it can be seen from Figs. 8, 9 and 10. However, we can discuss the overall performance with the following guidelines: a) The maximum values of the control inputs; b) The possible saturation of the control inputs for rejecting a disturbance; c) The tracking error in position and attitude; d) The dynamic energy index.

a) The maximum values of the control inputs: Solutions i and iii show the highest values at the third disturbance, however, the upper bound is not reached. These high values could be a problem due to the thrust saturation. On the other hand, the highest values of solution ii are lower than 70 Hz.

b) The possible saturation of the control inputs for rejecting a disturbance: Solution iii is the only design that saturates its inputs at the lower bound at the third disturbance, this leads to a loss in position and attitude as it can be seen in Figure 10.

c) The tracking error in position and attitude: Due to the lower robustness index, solution iii is not capable of rejecting the disturbances without losing its position and attitude. On the other hand, solution i and ii are capable of keeping their pose.

d) The dynamic energy index: Among the three solutions, solution iii was the one with the lowest value of the dynamic energy index. However, it can be noticed that this value is not very different from the one of the solution ii. The average value of the control inputs can give an insight of the energy consumption, solution i has an average around 62 Hz, solution ii has an average around 52 Hz and solution iii has an average around 48 Hz.

Among the three solutions, solution ii is the one that has the better trade-off between the two objectives according to the guidelines proposed. In order to show its response against disturbances, a simulation using the maximum perturbation applied to the hexa-rotor before becoming unstable was carried out. Furthermore, Gaussian noise was added to the measurements to have more realistic simulations, see Fig. 11.

VIII. CONCLUSIONS

A methodology to design a hexa-rotor capable of rejecting external disturbances was proposed. The use of tilted propellers allows having lateral forces that constitute an advantage over the standard hexa-rotors to mitigate external disturbances. We proposed two design indexes, the robustness index based on the radius of the maximum ball inscribed in the polytope of attainable forces and torques, and the energy index based on the control effort. These two indexes are shown to be opposed, hence, a multi-objective approach was adopted to solve the problem and to find the design that better trades-off with the two indexes. After solving the multi-objective problem with the help of an evolutionary algorithm, three solutions were taken to be analyzed in simulations. Some insights about the overall performance of the three design are given. Finally, we arrived at a design that has the better trade-off between the two indexes, this design was tested with the addition of Gaussian noise in the measurements and with the maximum allowable disturbance in order to show the feasibility of the methodology proposed and the design found.

REFERENCES

[1] D. Norris, *Build Your Own Quadcopter: Power Up Your Designs with the Parallax Elev-8*. New York, NY, USA: McGraw-Hill, 2014.

[2] K. P. Valavanis and G. J. Vachtsevanos, *Handbook of Unmanned Aerial Vehicles*. Springer, 2015.

[3] G. Heredia *et al.*, "Control of a multirotor outdoor aerial manipulator," in *Proc. IEEE/RSJ Int. Conf. Intell. Robots Syst. (IROS)*, Sep. 2014, pp. 3417–3422.

[4] J. R. Kutia, K. A. Stol, and W. Xu, "Canopy sampling using an aerial manipulator: A preliminary study," in *Proc. Int. Conf. Unmanned Aircraft Syst. (ICUAS)*, Jun. 2015, pp. 477–484.

[5] N. Staub, D. Bicego, Q. Sablé, V. Arellano, S. Mishra, and A. Franchi, "Towards a flying assistant paradigm: The OTHex," in *Proc. IEEE Int. Conf. Robot. Autom. (ICRA)*, May 2018, pp. 1–7.

[6] S. Waslander and C. Wang, "Wind disturbance estimation and rejection for quadrotor position control," in *Proc. AIAA Infotech Aerosp. Conf. AIAA Unmanned Unlimited Conf.*, 2009, p. 1983.

[7] R. Rashad, A. Aboudonia, and A. El-Badawy, "Backstepping trajectory tracking control of a quadrotor with disturbance rejection," in *Proc. 25th Int. Conf. Inf., Commun. Autom. Technol. (ICAT)*, Oct. 2015, pp. 1–7.

[8] C. Aguilar-Ibanez, H. Sira-Ramirez, M. S. Suarez-Castanon, and R. Garrido, "Robust trajectory-tracking control of a PVTOL under cross-wind," *Asian J. Control*, to be published.

[9] P. Segui-Gasco, Y. Al-Rihani, H.-S. Shin, and A. Savvaris, "A novel actuation concept for a multi rotor UAV," *J. Intell. Robot. Syst.*, vol. 74, nos. 1–2, pp. 173–191, 2014.

[10] M. Ryll, D. Bicego, and A. Franchi, "Modeling and control of FAST-Hex: A fully-actuated by synchronized-tilting hexarotor," in *Proc. IEEE/RSJ Int. Conf. Intell. Robots Syst.*, Oct. 2016, pp. 1–4.

[11] D. Brescianini and R. D'Andrea, "Design, modeling and control of an omni-directional aerial vehicle," in *Proc. IEEE Int. Conf. Robot. Autom.*, May 2016, pp. 3261–3266.

[12] S. Rajappa, M. Ryll, H. H. Bülthoff, and A. Franchi, "Modeling, control and design optimization for a fully-actuated hexarotor aerial vehicle with tilted propellers," in *Proc. IEEE ICRA*, May 2015, pp. 4006–4013.

[13] Y. Tadokoro, T. Ibuki, and M. Sampei, "Maneuverability analysis of a fully-actuated hexrotor UAV considering tilt angles and arrangement of rotors," *IFAC-PapersOnLine*, vol. 50, no. 1, pp. 8981–8986, 2017.

[14] G. Michieletto, M. Ryll, and A. Franchi, "Fundamental actuation properties of multirotors: Force–moment decoupling and fail–safe robustness," *IEEE Trans. Robot.*, vol. 34, no. 3, pp. 702–715, Jun. 2018.

[15] M. Henk, J. Richter-Gebert, and G. M. Ziegler, "16 basic properties of convex polytopes," in *Handbook of Discrete and Computational Geometry*. 2004, pp. 255–382.

[16] S. Boyd and L. Vandenberghe, *Convex Optimization*. Cambridge, U.K.: Cambridge Univ. Press, 2004.

[17] J. Vesterstrom and R. Thomsen, "A comparative study of differential evolution, particle swarm optimization, and evolutionary algorithms on numerical benchmark problems," in *Proc. Congr. Evol. Comput. (CEC)*, vol. 2, Jun. 2004, pp. 1980–1987.

[18] M. A. Panduro, C. A. Brizuela, L. I. Balderas, and D. A. Acosta, "A comparison of genetic algorithms, particle swarm optimization and the differential evolution method for the design of scannable circular antenna arrays," *Prog. Electromagn. Res. B*, vol. 13, no. 13, pp. 171–186, 2009.

[19] R. Storn and K. Price, "Differential evolution–A simple and efficient heuristic for global optimization over continuous spaces," *J. Global Optim.*, vol. 11, no. 4, pp. 341–359, 1997.

[20] E. Mezura-Montes, J. Velázquez-Reyes, and C. A. Coello-Coello, "A comparative study of differential evolution variants for global optimization," in *Proc. 8th Annu. Conf. Genetic Evol. Comput.*, 2006, pp. 485–492.

[21] J. Lampinen, "A constraint handling approach for the differential evolution algorithm," in *Proc. Congr. Evol. Comput.*, Washington, DC, USA, vol. 2, May 2002, pp. 1468–1473.

[22] K. Deb, "An efficient constraint handling method for genetic algorithms," *Comput. Methods Appl. Mech. Eng.*, vol. 186, nos. 2–4, pp. 311–338, 2000.

[23] T. P. Runarsson and X. Yao, "Stochastic ranking for constrained evolutionary optimization," *IEEE Trans. Evol. Comput.*, vol. 4, no. 3, pp. 284–294, Sep. 2000.

[24] G. J. Leishman, *Principles of Helicopter Aerodynamics With CD Extra*. Cambridge, U.K.: Cambridge Univ. Press, 2006.

[25] K. Deb, A. Pratap, S. Agarwal, and T. Meyarivan, "A fast and elitist multiobjective genetic algorithm: NSGA-II," *IEEE Trans. Evol. Comput.*, vol. 6, no. 2, pp. 182–197, Apr. 2002.

[26] E. A. Portilla-Flores, E. Mezura-Montes, J. Álvarez-Gallegos, C. A. Coello-Coello, and C. A. Cruz-Villar, "Integration of structure and control using an evolutionary approach: An application to the optimal concurrent design of a CVT," *Int. J. Numer. Methods Eng.*, vol. 71, no. 8, pp. 883–901, 2007.

[27] T. Lee, M. Leok, and N. H. McClamroch. (2010). "Control of complex maneuvers for a quadrotor UAV using geometric methods on SE (3)." [Online]. Available: https://arxiv.org/abs/1003.2005

VICTOR MANUEL ARELLANO-QUINTANA received the B.Eng. degree in industrial robotics engineering from the Instituto Politécnico Nacional, Mexico, in 2011, and the M.Sc. degree in automatic control, specializing in artificial neural networks, from Cinvestav-IPN, Mexico, in 2014. He is currently pursuing the Ph.D. degree with the Instituto Politécnico Nacional, working on design optimization of multirotors. His main interests are aerial robotics, design optimization, control, and identification, and artificial neural networks. He was the KUKA Innovation Award 2017 Finalist with the Tele-MAGMaS Team.

EDGAR ALFREDO PORTILLA-FLORES received the B.Sc. degree in electronics engineering from the Universidad Autonóma Metropolitana, Mexico, in 1992, the M.Sc. degree in mechanical engineering from the Instituto Tecnológico de Puebla, Mexico, in 2002, and the Ph.D. degree in electrical engineering from the Centro de Investigación y Estudios Avanzados, Mexico, in 2006. He was a Post-Doctoral Resident with the Universidade Estadual de Campinas, Brazil, in 2012. He is currently a full time Research Professor with the Centro de Innovación y Desarrollo Tecnológico en Cómputo, Instituto Politécnico Nacional, Mexico. His areas of interest are the optimum design of mechatronic systems and the application of bio-inspired algorithms to the solution of engineering problems. He is member of the National System of Researchers of Mexico.

EMMANUEL ALEJANDRO MERCHÁN-CRUZ received the B.Eng. degree in industrial robotics engineering and the M.Sc. degree in mechanical engineering, specializing in robotics, from the Instituto Politécnico Nacional, Mexico, in1998 and 2000, respectively, and the Ph.D. degree from The University of Sheffield, Sheffield, U.K., in 2005, after carrying out research on trajectory planning for multirobot manipulator systems. He is currently a Professor and an Academic Secretariat with the Instituto Politécnico Nacional, Mexico City. His main research interests are automatic systems, robotics, biomechanics, and process optimization. He is a member of the National System of Researchers of Mexico.